EVALUATION OF CANDIDATE METHODS FOR WELDING STEEL TO OTHER STRUCTURAL LIGHTWEIGHT METALS

Jerry E. Gould
Resistance and Solid-State Welding
EWI
Columbus, OH

Michael Eff
Friction Welding
Processes
EWI
Columbus, OH

Kate Namola
Resistance and Solid-State Welding
EWI
Columbus, OH

ABSTRACT

This paper addresses candidate technologies for attaching steels to selected lightweight materials. Materials of interest here include aluminum and titanium alloys. Metallurgical challenges for the aluminum-to-steel and titanium-to-steel combinations are first described, as well as paths to overcome these challenges. Specific joining approaches incorporating these paths are then outlined with examples for specific processes. For aluminum-to-steel joining, inertia, linear, and friction stir welding are investigated. Key elements of success included rapid thermal cycles and an appropriate topography on the steel surface. For titanium-to-steel joining, successful approaches incorporated thin refractory metal interlayers that prevented intimate contact of the parent metal species. Specific welding methods employed included resistance mash seam and upset welding. In both cases, the process provided both heat for joining and a relatively simple strain path that allowed significant bond line forging without rupture of the separating interlayer.

INTRODUCTION

Steel is and has been a primary construction material for many generations of military vehicles. Steels themselves can be formulated/processed to achieve unique combinations of strength, fracture toughness, corrosion resistance, etc. Over the past several decades, a range of other material systems have been commercially exploited in structural applications taking advantage of their unique combinations of properties. Specific classes of materials (aluminum alloys, titanium alloys) offer higher strength-to-weight ratios than commonly can be achieved with steels. Such systems are widely exploited for accomplishing vehicle weight reduction goals. The potential of combining these lightweight materials with conventional steels offers considerable flexibility in design and functionality of engineered structures. To that end, considerable effort has been placed on defining candidate welding and joining

technologies over the last few years. Not surprisingly, there is strong interest in application of these materials to military vehicle applications. Examples include aluminum-steel combinations for applications such as prop-shafts, gears, hulls, and ship transition joints. Potential titanium-to-steel combinations can be used for lightweighting both shafts and plate structures.

Welding of course implies intimate metallurgical interaction between the substrates to be joined. Each specific combination of metals offers a unique set of metallurgical challenges that must be addressed to achieve a successful welding method. Metallurgical issues in welding aluminum to steel are well understood [1-6]. These issues include differences in melting points, coefficients of both thermal expansion and conductivity, and most importantly, the potential for the formation of a range of intermetallics. Previous work has suggested that the most deleterious intermetallic compounds include the Al_2Fe_5 and $AlFe_2$ stoichiometries [1,5,6]. Such intermetallics are associated with low strength–low ductility fractures along the bond lines in the developed joints.

Welding for the titanium-to-steel combination has a different set of metallurgical challenges. A major feature of the titanium/iron combination is the formation of low-melting eutectics. The deepest of these eutectics occurs at 1,085°C, corresponding to a melting point suppression of about 600°C and 500°C for the titanium and steel sides of the joint, respectively. Nickel (present in austenitic grades of stainless steels) offers additional melting point suppression. For fusion processes, such melting point suppression implies solidification and liquation cracking concerns. The latter (liquation cracking) is even possible with solid-state welding processes. Further, welding steels to titanium alloys (Ti-alloys) typically results in an array of intermetallic compounds that includes TiFe, $TiFe_2$, and for

stainless steels, the additional formation of TiNi, $TiNi_3$, and σ-phases [7].

Obviously, design and selection of welding processes for specific material combinations must take such metallurgical reactions into consideration. Below, separate classes of joining processes are described for two dissimilar metal combinations. These include the use of friction welding for joining aluminum to steel, and interlayer-based forge welding approaches for attaching titanium to steel.

FRICTION-BASED PROCESSING FOR ALUMINUM-TO-STEEL JOINTS

As suggested above, the key to successful welding of aluminum to steel is attachment without formation of the associated intermetallic compounds. Considerable previous research [5,8,9] has shown that the kinetics of intermetallic formation largely define processes and practices for creating such joints. Essentially, reduced processing temperatures and times both retard the kinetics of intermetallic formation. For friction welding, increased contact forces lead to reduced temperatures in the joint, which related to the metal yield strength as a function of temperature.

The variation in yield strength as a function of temperature for Al 6061 is shown in Figure 1 [10]. It can be seen that the higher the applied stress, the lower the temperature at which the aluminum will forge across the steel interface. Reduced times at temperature can be achieved through reducing effective friction times.

A final element of successful friction welding between aluminum and steel is preparation of the steel interface itself. This preparation includes facing the steel soon before welding, and providing a profile on that surface. Facing the surface immediately before welding minimizes iron oxides that inhibit bonding. The profile is beneficial in that it provides a torturous path at the

Evaluation of Candidate Methods for Welding Steel to Other Structural Lightweight Metals, Gould, et al.

Page 2 of 11

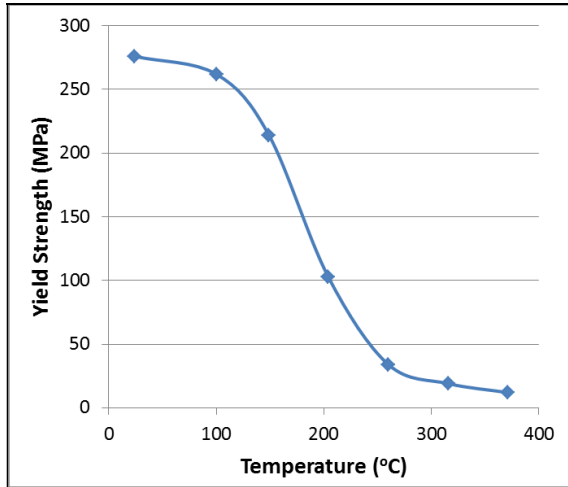bond line increasing the energy of fracture at this location.

Figure 1: Yield strength as a function of temperature for an Al 6061-T6 alloy [10].

The rotary variant of friction welding is the best established for joining aluminum to steel and has been used on production automotive components for decades. Recently, welding of nominally thick wall components has been demonstrated using the inertia variant of rotary friction welding. The components of interest included Al 6061 and 1020 steel tubes, nominally 127 mm in diameter with a 10-mm wall thickness.

Best practices included a machined surface topography, high contact forces, and rapid deceleration times. Resulting process waveforms are seen in Figure 2. Note that the contact stresses are a very high fraction of the yield strength, suggesting reduced forging temperatures. In addition, note that the deceleration (heating times) are also short, on the order of 200 ms.
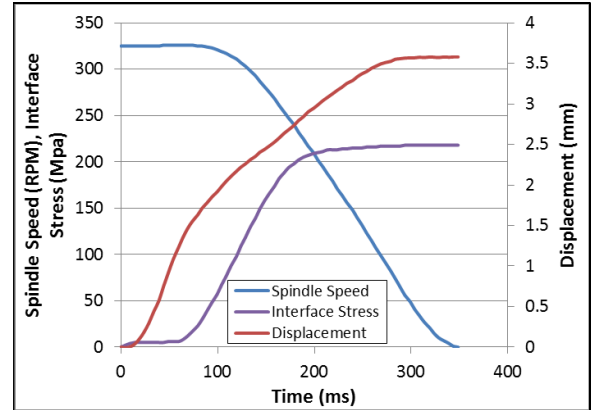

Figure 2: Spindle speed, contact stress, and platen displacement when inertia welding an aluminum-to-steel joint.

The joint itself is shown in Figure 3. These joints showed tensile strengths in excess of 300 MPa, with failures in the aluminum heat-affected zones (HAZ). A section through the fracture area of a tensile specimen from a weld made at the above conditions is provided in Figure 4. The section clearly shows the profile of the topography applied to the steel, as well as the failure through the aluminum in the soft region of the HAZ.

Figure 3: Finished large diameter/heavy wall aluminum to steel inertia weld. Part has a 127-mm diameter and 10-mm wall.

Evaluation of Candidate Methods for Welding Steel to Other Structural Lightweight Metals, Gould, et al.
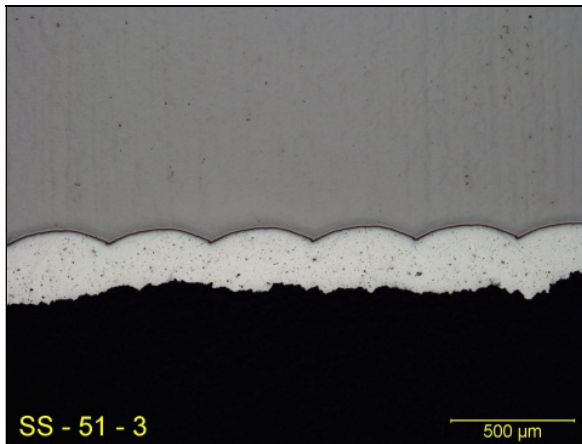
Page 3 of 11

Figure 4: Cross section through a tensile tested specimen from an aluminum-to-steel inertia weld. Note the textured surface on the steel and failure in the aluminum HAZ.

Figure 5: A LFW aluminum-to-steel specimen. The bar stock is 17 mm and the working interface is 12×12 mm.

Linear friction welding (LFW) is also being investigated for aluminum-to-steel joints. The equipment used was a dedicated mechanical drive system manufactured by APCI. This system has been described elsewhere, but is unique in that translational forces (and amplitudes) are created by a programmable cam and flywheel arrangement.

Joining trials were again done between an Al 6061-T6 alloy and a 1018 steel. Material was purchased as nominal 17-mm diameter bar stock, with working faces 12×12 mm machined on both components for welding. Welding trials were based on previous rotary work. A resulting joint is shown in Figure 5. Sample process waveforms are provided in Figure 6. The plot provides variations in platen displacement, interface stress, and translational amplitude through the welding process. It is of note that the data presented shows a noise level characteristic of the translational frequency used. In many ways, the plot is similar to that shown for inertia welding above.
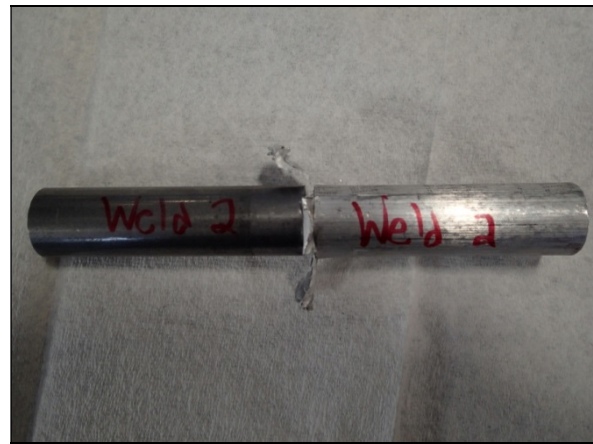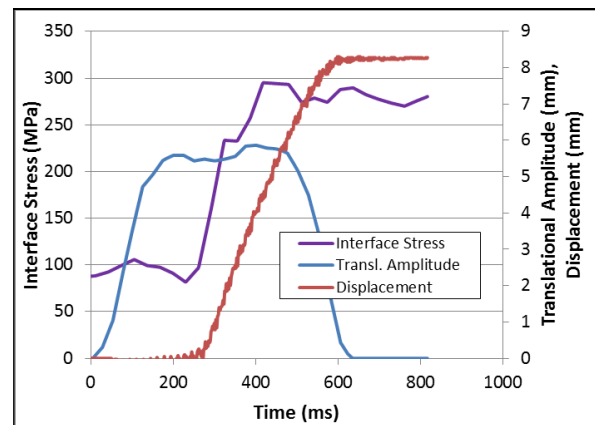

Figure 6: Interface stress, translational amplitude, and platen displacement for a LFW aluminum-to-steel joint.

Resulting microstructures are similar to those seen in the inertia welds. An optical micrograph showing the interrelation between the steel surface and the forged aluminum is provided in Figure 7. Of note, even though no surface texture was purposefully applied, machining the steel face obviously left a series of striations nominally 40-μm wide by 10-μm deep. Clearly, a layer of aluminum adjacent to this topography is of different contrast. It is suspected this is a region of higher deformation in the aluminum driven by that steel surface morphology.
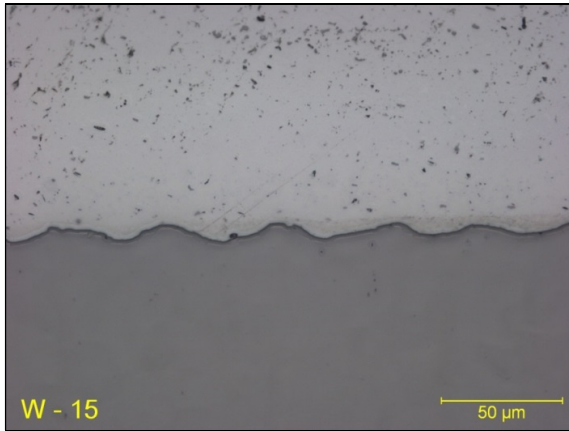
Evaluation of Candidate Methods for Welding Steel to Other Structural Lightweight Metals, Gould, et al.

Page 4 of 11

Figure 7: Optical micrograph of the weld interface in an aluminum-to-steel linear friction weld. Note deformation zone in the aluminum.

Further work was done to examine for any intermetallic formation in these joints. A higher resolution scanning electron microscopy (SEM) image of the joint area is provided in Figure 8. This figure indicates little or no intermetallic compounds along the bond line. At best, there may be some scattered Al-Fe-type intermetallics as particles imbedded in the aluminum matrix.
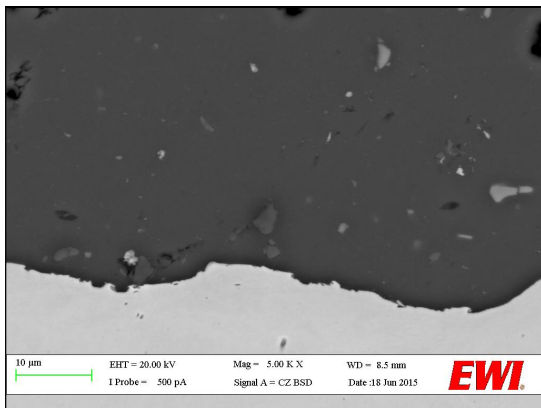

Figure 8: Backscatter SEM image from the interface in an aluminum-to-steel LFW. Note lack of intermetallics along the bond line.

These observations suggest that if intermetallics formed as a result of LFW, severe local deformation in the aluminum extracted them from the surface with resulting dispersion into the forged material. Tensile testing from sample

joints showed failure strengths in excess of 300 MPa. This result is comparable with the inertia welds described above, as well as the attached Al 6061 base metal itself.

LFW has also been examined for this specific material combination. In these trials, Al 6061-T6 and 1018 steel were joined together in a butt configuration. Welding was performed with a novel low aspect ratio/zero tilt tool. The tool is shown schematically in Figure 9. For welding, the tool was offset into the aluminum at a position where the pin would just scarf the steel surface. The aluminum plate was also shimmed to sit relatively 0.25 mm above the top steel surface to prevent the tool shoulder from wearing on the steel surface. The rotation direction allowed the advancing side of the tool to scarf the steel surface. The resulting weld is shown in Figure 10. Note that at the exit hole, the pin is barely in contact with the steel side of the joint. Resulting joints showed strengths on the order of 200 MPa and failed in the aluminum HAZ.
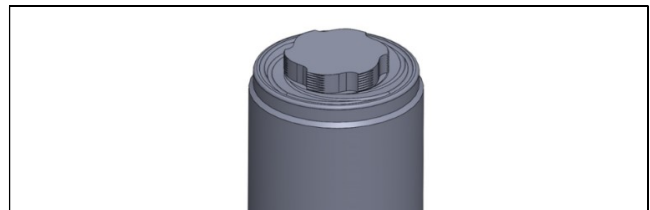

Figure 9: Schematic representation of the friction stir tool used in these studies. Pin length is 3 mm.
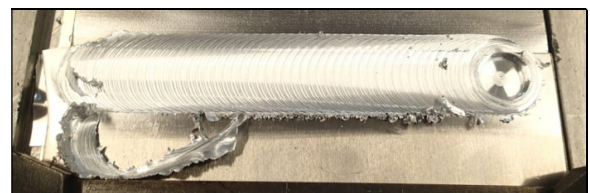

Figure 10: Friction stir weld between aluminum and steel. Note the offset of the tool into the aluminum side of the joint.

The macrostructure of the resulting joint is shown in Figure 11. This is a backscatter SEM image, allowing straightforward discernment

Evaluation of Candidate Methods for Welding Steel to Other Structural Lightweight Metals, Gould, et al.

Page 5 of 11

between the aluminum and steel. It is evident from this image that the scarfing provided by the tool results in a surface topography similar to that seen in the inertia and LFW data above. The resulting topology shows a period of about 350-μm and 100-μm deep. The aluminum is in full intimate contact with this surface. There is also evidence of aluminum at the top surface of the steel, related to the initial vertical offset used.
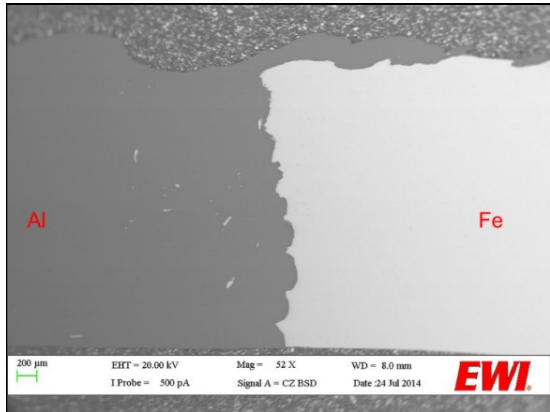

Figure 11: SEM backscatter image showing the macrostructure of an aluminum-to-steel friction stir weld.

Additional detail of the actual bond interface is provided in Figure 12. This again is an SEM backscatter image. Of interest here is that the aluminum has dark and the steel light contrast. However, there is an intermediate contrast phase at the contacting surfaces, presumably an intermetallic phase(s). That intermetallic phase appears to be extensive in these friction stir welds. This difference (from the inertia and linear friction welds) is undoubtedly due to the significantly longer thermal cycles associated with FSW. This longer thermal cycle would account for both the observations of intermetallic compounds, as well as the lower mechanical properties in the aluminum HAZ.
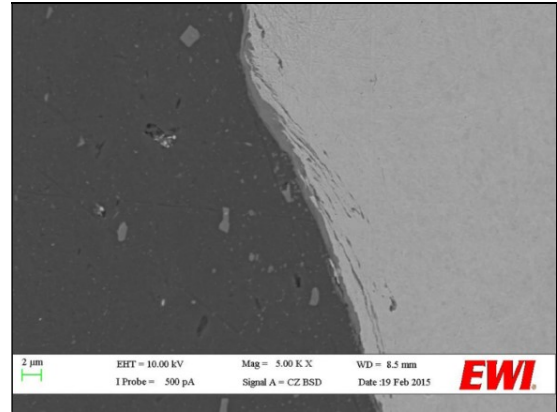

Figure 12: SEM backscatter image showing the details of the aluminum-to-steel interface in a friction stir weld. Note the intermetallic at the bond line.

JOINING OF STEEL TO TITANIUM WITH INTERLAYERS

The key to successful joining of titanium and its alloys to steels, based on the discussion above, is to maintain chemical separation of the substrates throughout the process. To achieve effective joining, the process must be capable of bonding each of the substrates to the interlayer, and allow the interlayer to maintain its integrity. For example, explosion bonding has been done with copper, Monel®, and tantalum interlayers [11-13]. Resistance-based, solid-state welding methods offer considerable opportunity for accomplishing these objectives. Such processes facilitate simple (one or two dimensional) strain paths, that allow deformation without tearing of the interlayer. In addition, the heat and strain associated with these processes facilitates solid-state joints between each of the substrates and the interlayer.

Resistance mash seam welding (RMSeW) has been demonstrated for creating sheet metal based titanium-to-steel joints. For this process, sheet metal parts are configured with a small overlap (typically 1-3 times the metal thickness) in a resistance seam welding machine. Current is passed between the wheels, which are in turn rolled along the bond line. Resistance heating from the current combined with the force from the

Evaluation of Candidate Methods for Welding Steel to Other Structural Lightweight Metals, Gould, et al.

Page 6 of 11

weld wheels themselves creates a continuous forge joint.

In the work described here, a nominal 3.5-mm CP Ti sheet was bonded to a 3.0-mm 304SS. Of note for this process, a 15-degree bevel was machined on the steel. The locating the edge of the CP Ti sheet at the center of this bevel. All joints included a 63-μm thick niobium (Nb) foil between the components located prior to welding. The resulting joint is shown in Figure 13. This figure shows complete set-down of the CP Ti against the steel. Also, the edge of the Nb foil can be seen extending from the bond line between the substrates.
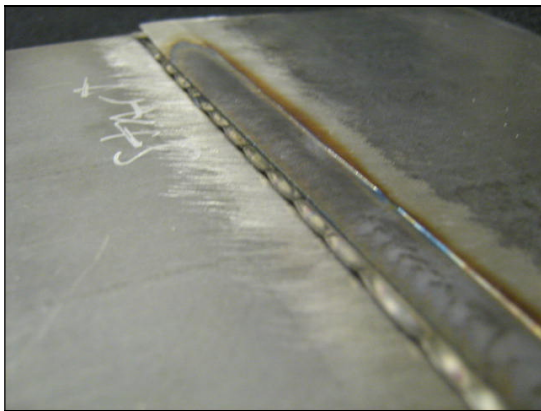

Figure 13: Top surface of an RMSeW made between 304SS and Ti sheet. The top sheet is the 304SS, and the residual Nb interlayer can be seen.

A macrograph of the resulting joint is shown in Figure 14. Here the CP Ti sheet is located on the top. It can be seen that the CP Ti essentially forges along the surface defined by the bevel on the stainless steel. In addition, the foil interlayer can be seen to be continuous across the bond surface. It is also evident that both the CP Ti and the 304SS have effectively bonded to the foil over the majority of the interface. The only lack of bonding evident is at the edges where the forging CP Ti has lost constraint against the stainless steel.
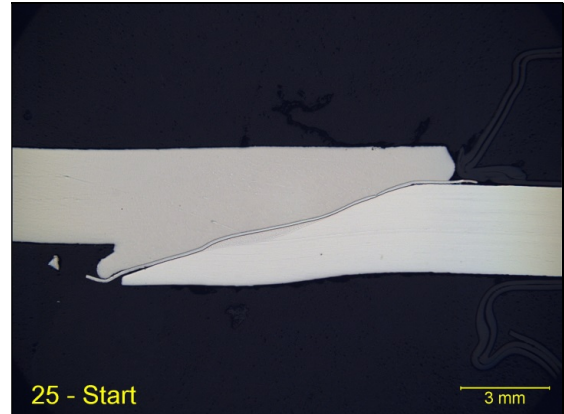

Figure 14: Cross section of the RMSeW between 304SS and Ti. Note the residual interlayer across the bond line.

Some details of the interlayer morphology following joining is provided in Figure 15. This is a SEM image of the bond line roughly 2 mm from the lower edge of the specimen. Also included on this micrograph are scans showing the distribution of Fe (from the stainless steel), Ti (from the CP Ti), and Nb (from the interlayer). This micrograph shows the interlayer has retained a thickness of roughly 60 μm and that the compositions clearly delineate where the different species come into contact.
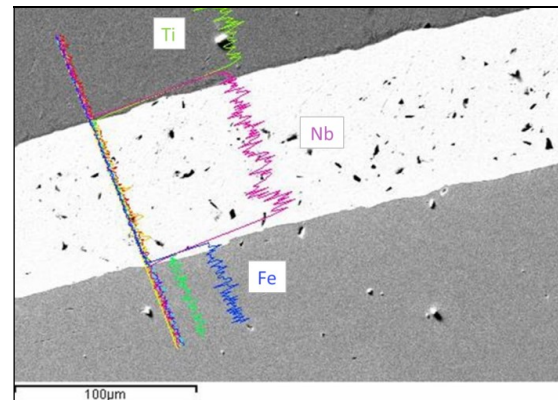

Figure 15: Details of a Ti-to-SS RMSeW. Note complete chemical separation of the substrates by a nominally 60-μm layer of Nb.

Occasionally, the interlayer was observed to rupture. A SEM image of one such rupture is shown in Figure 16. The location of this rupture is

Evaluation of Candidate Methods for Welding Steel to Other Structural Lightweight Metals, Gould, et al.

Page 7 of 11

about 2 mm from the lower edge of the bond line of a different (from above) specimen. The effect of interlayer breakdown is evident. Where the substrates have come into contact, melting has instantly occurred. The relative chemistry is indicated by the Ti and Fe scans also included in Figure 16. These scans suggest the titanium-rich liquid phase that is consistent with the low melting Ti-Fe eutectic (1,085°C melting temperature). Melting in this temperature range is consistent with the anticipated (RMSeW) forging temperatures of both the CP Ti and the stainless steels.
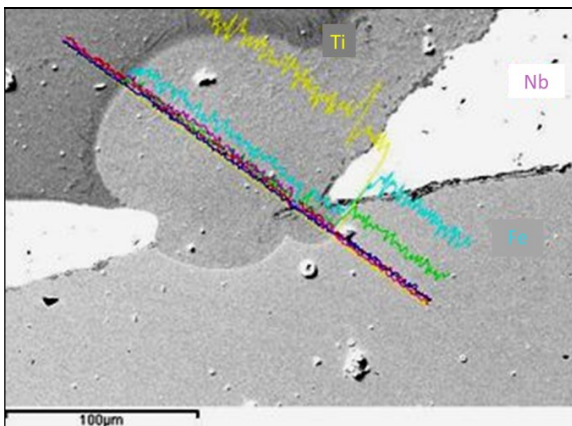

Figure 16: Microstructural and chemical variations along the bondline where the interlayer has ruptured. A pool of eutectic has formed at this location.

Mechanically, triplicate transverse tensile testing of these joints showed strengths between 200 and 300 MPa. Failures were consistently in the CP Ti at the joint edge. Triplicate guided bend tests on similar joints showed fiber strains at failure in excess of 10%.

Ongoing work is investigating the use of such refractory metal interlayers for upset welding (UW) titanium to steel. UW is a resistance-based forge-welding process. The process is to produce butt joints on either sheet or bar type workpieces. In this process, workpieces are configured in a press-type frame and brought under force, and a current is applied. The workpieces resistance heat

and, upon reaching the upsetting temperature, are forged together. An example of an upset weld made on 6-mm thick Ti-6Al-4V is shown in Figure 17. The material displaced during upsetting is readily seen. In this study, Ti-6Al-4V is joined to a 304SS. The cross section for both materials was nominally 6×25 mm. The interlayer material was again Nb, nominally 60-μm thick. For joining, the Nb foil was pre-attached to the faying surface of the Ti-6Al-4V prior to welding using a small capacitive discharge based system.
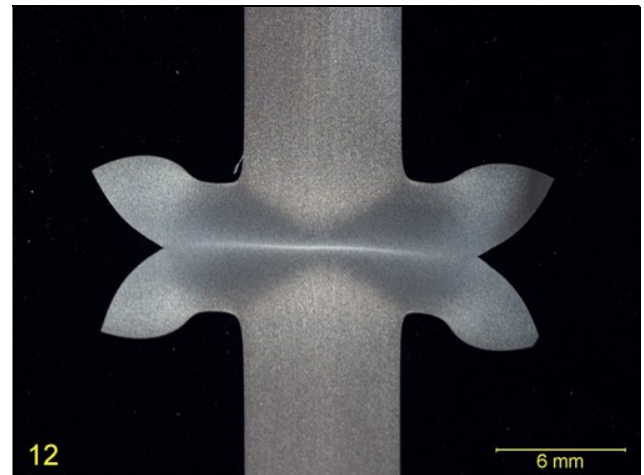

Figure 17: Cross section of an upset weld made on 6-mm Ti-6Al-4V sheet. Note the flash extrusion from both workpieces.

The macrostructure of the resulting joint is shown in Figure 18. As evident from this macrograph, the forging is decidedly biased toward the Ti-6Al-4V. However, there is also clear evidence of deformation on the 304SS side of the joint. Further, the thin Nb foil can also be seen extending from the top and bottom surfaces at the bond location. The combination of heat and surface strain on both sides of the Nb foil allows two solid-state joints to form, similar to that seen in the RSMeW welds discussed above.
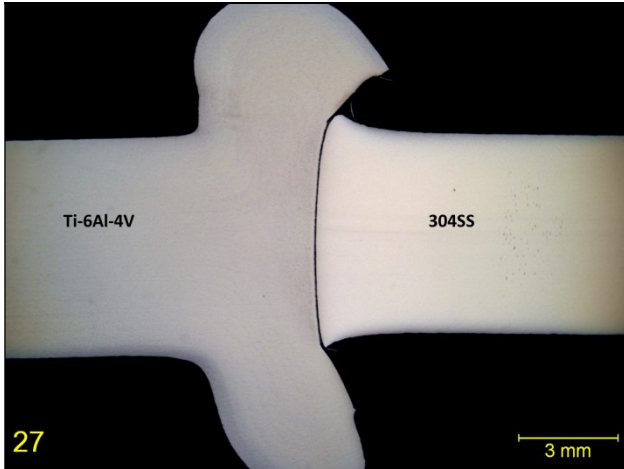
Evaluation of Candidate Methods for Welding Steel to Other Structural Lightweight Metals, Gould, et al.

Figure 18: Cross section of an upset weld made between Ti-6Al-4V and 304SS employing a Nb foil at the interface.

Figure 19: Details of the bond line microstructure for a Ti-6Al-4V-to-304SS upset weld using a Nb interlayer. Micrograph is taken near the center of the weld.

Figure 20: A lack of bond incident at the edge of the Ti-6Al-4V to 304SS upset weld using a Nb interlayer. Note preferential bonding to the 304SS.

Details of the bondline structure are provided in Figures 19 and 20. Figure 19 provides a higher magnification view of the joint interface at the center of the sample. The integrity of the bonding of the Nb foil between both the Ti-6Al-4V and the 304SS is evident. Of note, the bond line on the Ti-6Al-4V side of the joint is considerably less distinct than that on the 304SS side. It is believed that this is due to the relative miscibility of Nb and Ti at high temperatures (above the β-transus) promoting a component of diffusion bonding. The residual interlayer of the interlayer appears to be about 50 μm, compared to an original thickness of about 60 μm.

The combination of interlayer thinning and continuity suggests that the Nb can be effective with considerable application of bond line strain. Some dis-bond, however, was noted at the edges of the contact area. An example is shown in Figure 20. This image is a lower magnification micrograph compared to that shown in Figure 19. Dis-bond between the Nb interlayer and the Ti-6Al-4V substrate can be seen over the last 400 μm of bond length. Improved upset on the 304SS side of the joint would greatly minimize such intrusions.
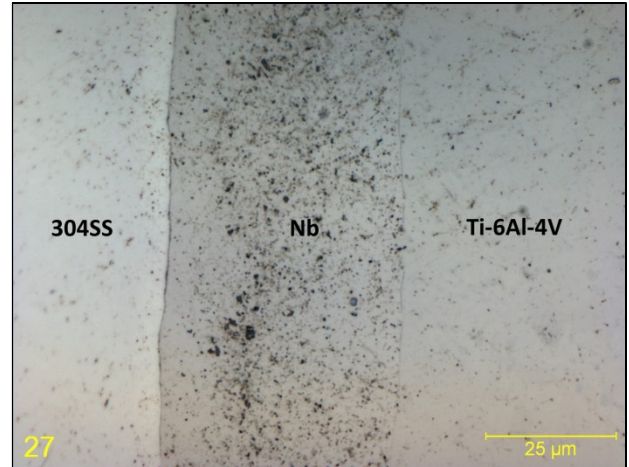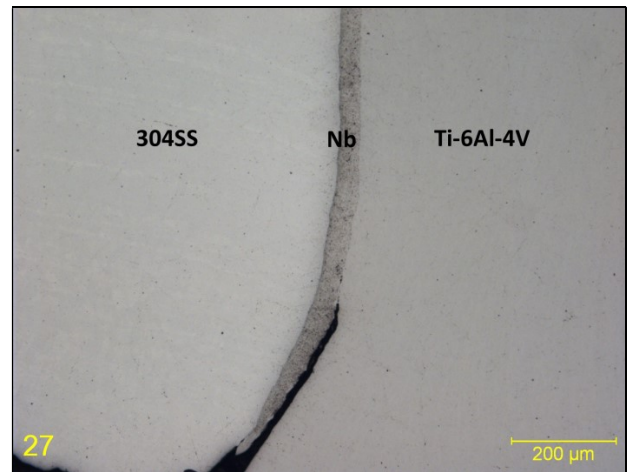
Strengths for these joints are currently on the order of 200 MPa. Continued process optimization will be required to achieve strengths comparable to the Ti-6Al-4V and 304SS base materials.

SUMMARY

Definition and development of appropriate joining technologies for dissimilar metal combinations clearly requires an understanding of potential interactions of the substrate species. By

Evaluation of Candidate Methods for Welding Steel to Other Structural Lightweight Metals, Gould, et al.

Page 9 of 11

understanding these interactions, joining processes can be selected and developed that can minimize or avoid these interactions. In this work, two classes of dissimilar metal joints are described, along with candidate process solutions. The dissimilar metal combinations included aluminum to steel and titanium to steel. Aluminum-to-steel joining is largely challenged by the formation of deleterious intermetallic compounds at the bond line. Successful process solutions have included those that provided two features to the final joint microstructure. These features included providing a sufficiently rapid thermal cycle to avoid nucleation of intermetallic compounds and a tortuous interface geometry that increased required energies for crack propagation. Examples of technologies that exploit these features include inertia, linear, and FSW. The first two are most successful when heat times are maintained under a few hundred milliseconds and a topography is applied to the steel surface. The latter is most successful when the stir tool itself can provide the topography to the steel surface.

Titanium-to-steel joining is challenged by the formation of low-melting eutectics, as well as a range of intermetallic compounds. The former can result in both solidification and liquation cracking in the fusion and HAZs, respectively. For this combination of materials, processes have been developed that include a barrier to prevent intimate contact between the substrates. Here, solid-state or forge welding processes combined with use of refractory metal-based interlayers have been employed. Two variants of solid-state welding Ti-alloys to 304SS with a Nb foil interlayer were described. These processes included RMSeW and UW. In both cases, the processes provided heat and a relatively simple strain path at the bond line. The time at temperature promoted softening and forging of the joint components (Ti-alloy, Nb interlayer, 304SS) and a simple strain path that allowed extension of the foil without rupture. These features allowed

solid-state bonding of the Nb foil to both the Ti-alloy and 304SS substrates, allowing joining without intimate contact between the two metal species. It was noted that when the foil did rupture, temperatures in the joint were sufficient to cause constitutional melting. This effect would inevitably compromise the integrity of the joint.

REFERENCES

[1] C.E. Albright, "The Fracture Toughness of Steel–Aluminum Deformation Welds", Welding Journal Research Supplement, vol 60, issue 11, pages 207s-214s, 1981.

[2] I.A. Chernenko, V.R. Ryabov, A.V. Reshetnyak, A.N. Muraveinik, and I.A. Dzykovich, "Friction Welding AD1 Aluminum to 12Kh18N10T Steel" Welding International, vol 3, issue 7, pages 586-590, 1989.

[3] F. Haddadi, "Rapid Intermetallic Growth under High Strain Rate Deformation during High Power Ultrasonic Spot Welding of Aluminium to Steel", Materials & Design, vol 66, issue 2, pages 459-472, 2015.

[4] H.J. Park, et al., "Joining of Steel to Aluminum Alloy by AC Pulse MIG Welding", Materials Transactions, vol 50, issue 9, pages 2314-2317, 2009.

[5] E. Taban, J.E. Gould, and J.C. Lippold, "Dissimilar Friction Welding of 6061-T6 Aluminum and AISI 1018 Steel: Properties and Microstructural Characterization", Materials & Design, vol 31, issue 5, pages 2305-2311, 2010.

[6] H. Pringer, et al., "On the Formation and Growth of Intermetallic Phases during Interdiffusion between Low-Carbon Steel and Aluminum Alloys", Acta Materialia, vol 59, issue 4, pages1586-1600, 2011.

[7] T.B. Massalski, editor in chief, "Binary Phase Diagrams", American Society for Metals, Metals Park, OH, 1990.

[8] E. Taban, J.E. Gould, and J.C. Lippold, "Characterization of 6061-T6 Aluminum

Evaluation of Candidate Methods for Welding Steel to Other Structural Lightweight Metals, Gould, et al.

Page 10 of 11

Alloy to AISI 1018 Steel Interfaces during Joining and Thermo-Mechanical Conditioning", Materials Science and Engineering A – Structural Materials Properties Microstructure and Processing, vol 527, issues 7-8, pages 1704-1708, 2010.

[9] C.Y. Lee, et al., "Dissimilar Friction Stir Spot Welding of Low Carbon Steel and Al-Mg Alloy by Formation of IMCs", Science and Technology of Welding and Joining, vol 14, issue 3, pages 216-220, 2009.

[10] "Metals Handbook, Vol.2 - Properties and Selection: Nonferrous Alloys and Special-Purpose Materials", ASM International 10th Ed, 1990.

[11] J.G. Banker and V.D. Linse, "Explosion Welds between Titanium and Dissimilar Metals. Advances in the Science and Technology of Titanium Alloy Processing", TMS, Warrendale, PA, 1997.

[12] Y.L. Trykov, V.N. Arisova, S.A. Volobuev, and A.F. Trudov, "Structure and Properties of a Titanium-Steel Composite Produced by Explosion Bonding", Welding International, vol 12, issue 2, pages 127-130, 1998.

[13] B. Kosec L. Kosec, G. Cevnik, P. Fajfar, M. Gojic, and I. Anzel, "Analysis of Interface at Explosive Welded Plates from Low-Carbon Steel and Titanium", Metalurgija, vol 43, issue 2, pages 83-86, 2004.

Evaluation of Candidate Methods for Welding Steel to Other Structural Lightweight Metals, Gould, et al.

Page 11 of 11